

Riding the Shifting Potential: When Reactive Control Suffices for Multi-Goal Behavior

Vito Mengers^{1,2}

Oliver Brock^{1,2,3}

Abstract—Reactive control is often considered insufficient for multi-objective tasks because conflicting objectives give rise to local minima. We argue this limitation is not inherent but arises from static encodings that fail to reflect how objectives currently interact. We exploit the interaction structure encoded in a graph-based world model by extending it with nullspace projections: conflicts are resolved where they arise by projecting lower-priority gradients into the nullspace of higher-priority ones, with priorities determined continuously from the current state. We demonstrate this in two domains where conflicts between objectives are central: navigation around non-convex obstacles, where static potential fields fundamentally fail, and planar pushing of non-convex objects, where our method achieves 100% success across one-hundred configurations versus 0% for the steepest-descent baseline and ~55% for diffusion policy, without demonstrations or retraining. The same formulation transfers directly to a real robot with additional perceptual and kinematic constraints, accommodating them through the same mechanism.

I. INTRODUCTION

Robotic behavior is often understood through a division between planning and control. Planning is invoked when tasks involve multiple, potentially conflicting objectives, as it can anticipate future interactions and explicitly order subgoals [1]–[3]. Control, by contrast, operates locally and reactively [4,5], and is therefore typically regarded as insufficient for such tasks [6,7]. This view implicitly attributes the need for planning to the complexity of the task itself.

In this paper, we revisit this assumption. We argue that the primary difficulty in multi-objective behavior does not lie in task complexity per se, but in how relationships between objectives are represented. Local minima, commonly cited as a fundamental limitation of reactive methods [7]–[10], arise not primarily from the task structure, but from static encodings that fail to reflect how objectives currently interact. The structure of the world encodes this interaction: gradients propagating through a model of the world toward actuation signals reveal whether objectives reinforce, are orthogonal, or conflict—and this information changes as the state changes. Reading it locally is sufficient to coordinate between objectives, provided conflicts arise from currently active objectives

rather than interactions that only emerge through future state sequences, as in Tower of Hanoi or a Rubik’s Cube [11,12].

Recent work [13] encodes world structure in a graph and showed that propagating gradients through it is sufficient to solve sequential, multi-step tasks without planning. However, when multiple gradients must be followed simultaneously, whether from distinct objectives or from competing paths toward the same one, they may conflict. These conflicts give rise to local minima that myopic gradient following cannot escape [13].

We address this by extending the same graph-based representation, Active InterCONnect (AICON) [13,14], with nullspace projections [15]. Rather than selecting a single gradient, we resolve conflicts where they arise in the graph: the nullspace of each gradient defines directions along which other objectives can be pursued without interference, i.e., without worsening the higher-priority objective, and priorities are determined continuously from the current interaction structure rather than fixed in advance. When no instantaneous combination resolves a conflict, the nullspace provides a direction for exploration until the interaction structure changes. This prevents many local minima from forming and provides a mechanism to escape them when they do—without anticipating future interactions or committing to a priori priority orderings.

We demonstrate these ideas in two domains where simultaneous conflicts between objectives are central: navigation around non-convex obstacles, where goal and avoidance gradients directly oppose each other (Sect. IV), and planar pushing of non-convex objects, where beneficial and detrimental contacts create irresolvable conflicts under myopic gradient selection (Sect. V). Both are practically unsolvable by the steepest-path strategy of [13] and are typically addressed through planning [8,16] or compressed anticipation in a learned policy [17]. We show that behavior in these domains can instead be produced reactively within a single unified representation that jointly handles perception, action selection, and conflict resolution—and that extending it to a real robot with additional constraints, such as partial observability and joint limits, requires only adding new estimators and goals to the same graph, without modifying existing components.

Taken together, these results question whether the boundary between planning and control reflects the structure of the problem or merely the limitations of how objectives have historically been represented. Once static encodings are replaced by representations that evolve with the state and resolve conflicts as they arise, the distinction loses

¹ Robotics and Biology Laboratory, Technische Universität Berlin

² Science of Intelligence (SCIoI), Cluster of Excellence, Berlin, Germany

³ Robotics Institute Germany

We gratefully acknowledge funding by the Deutsche Forschungsgemeinschaft (DFG, German Research Foundation) under Germany’s Excellence Strategy – EXC 2002/1 “Science of Intelligence” – project number 390523135. This work has been partially supported by the German Federal Ministry of Research, Technology and Space (BMFTR) under the Robotics Institute Germany (RIG).

much of its necessity. A broad class of behaviors previously thought to require planning can instead be understood as arising from continuously adapting interactions between objectives—interactions that planning anticipates statically, but that reactive control, given the right representation, can resolve online. This perspective connects robotic behavior generation to more general principles in optimization and biological control (Sect. VI), where resolving competing influences is a central concern.

II. RELATED WORK

Approaches to multi-objective robotic behavior span planning (Sect. II-A), learned policies (Sect. II-B), and control (Sect. II-C). While both planning and learning can coordinate subgoals, they often lack the ability to react to disturbances not anticipated or not reflected in the data. Control methods are inherently reactive and robust but often prone to local minima unless supported by hand-engineered hierarchies, switching logic, or heuristics. We build on control, extending it to resolve conflicts between simultaneous objectives online and avoid minima—without planning, fixed hierarchies, or retraining.

A. Planning

Classical planning [1,18], task and motion planning [2,3], and trajectory optimization [19] explicitly balance multiple objectives, but require accurate models and often become prohibitively slow as task complexity grows. For long-horizon problems they frequently serialize subgoals or offload conflict resolution to the skill level [2,18,20], effectively sidestepping the underlying multi-goal challenge. Extensions using large language or vision-language models to replace slow search still rely on sequencing tasks [21,22], but require anticipating all relevant interactions in advance. As a result, they remain brittle in dynamic and uncertain environments due to their limited reactivity.

B. Learned Policies

Reinforcement [23] and imitation learning [17] instead encode goal trade-offs within a single policy, enabling smooth execution and robustness to error cases represented in the data. However, once trained, these trade-offs are fixed: changing priorities or constraints typically requires costly retraining [24]. Moreover, learned policies often behave like high-dimensional lookup tables of their training data [25], making them brittle to novel goal combinations and environmental changes [24,26].

C. Control Methods

Reactive control exploits local gradient information [5], offering robustness and low computational cost. However, conflicting goals can create local minima that prevent progress [8]. Heuristics such as wall-following or prioritized avoidance mitigate this only in narrow settings [27, 28]. Hierarchical schemes or transition structures such as subsumption [4], state machines [29], behavior trees [29], nullspace control [15], or Riemannian Motion Policies [30]

improve compositionality but impose fixed hierarchies that must be hand-engineered, effectively hard-coding a policy. Recent work [13] showed how making the potential field adaptive can avoid minima in sequential tasks yielding robust behavior, but simultaneous goals still interfere.

In contrast, our work extends these adaptive potential fields to the simultaneous setting. By projecting gradients into one another’s nullspaces and dynamically adjusting priorities, we resolve conflicts, escape local minima, and retain the robustness of reactive control—without the anticipatory rigidity of planning or the fixed trade-offs of learned policies.

III. ADAPTIVE NULLSPACE PROJECTIONS IN AICON

Active InterCONnect (AICON) is a framework for encoding regularities between sensory inputs (S), actions (A), and time (t) through state-dependent active interconnections among system components. By representing the world as a graph of recursive estimators coupled through differentiable interconnections, it supports robust perception [14], active sensing, and sequential behavior without planning [13] within a unified representation. Here, we extend this framework to resolve conflicting simultaneous objectives through nullspace projections, addressing the fundamental limitation of myopic gradient descent when goals are in conflict.

We first summarize how AICON encodes and leverages world regularities for perception and action (Sect. III-A), then introduce nullspace projections (Sect. III-B), and finally show how these projections dynamically resolve conflicts, preventing (Sect. III-C) and escaping (Sect. III-D) local minima while maintaining control stability (Sect. III-E).

A. Encoding Regularities for Perception and Action

AICON represents the structure of the world by encoding regularities in $S \times A \times t$. This is achieved through components that estimate relevant quantities $\mathbf{x}_1, \mathbf{x}_2, \dots, \mathbf{x}_N$ of the world state and *active interconnections* that couple them. Each component functions as a recursive estimator, updating its internal state \mathbf{x} based on sensors and actuators as well as constraints from the interconnections. These interconnections are differentiable and state-dependent, enabling bidirectional information flow between components.

Goals are expressed as differentiable scalar cost functions $g(\mathbf{x})$ defined over a component’s estimate \mathbf{x} . Gradients of these goals can be propagated backward through the network of interconnected estimation components using the chain rule (Eq. (1)) along a path $\mathbf{p} : g \rightsquigarrow \mathbf{a}$ until they reach actuation signals \mathbf{a} . In this way, AICON interprets the encoded regularities in components and interconnections as actionable information: descending the goal gradient produces closed-loop behavior grounded in perception.

$$\nabla_{\mathbf{a}}^{\mathbf{p}} g = \frac{\partial g(\mathbf{x}_1)}{\partial \mathbf{x}_1} \frac{\partial \mathbf{x}_1}{\partial \mathbf{x}_2} \dots \frac{\partial \mathbf{x}_{N-1}}{\partial \mathbf{x}_N} \frac{\partial \mathbf{x}_N}{\partial \mathbf{a}} \quad (1)$$

Because interconnections are state-dependent and gradients can propagate along multiple paths through the network, the resulting gradient expansion naturally reveals subgoals: adjustments that change the regime of an interconnection and

thereby enable further progress toward the goal. In this way, we obtain a gradient from each path $p \in \mathbb{P}$ connecting the goal g to an actuation signal \mathbf{a} . These gradients represent both direct routes toward the goal and intermediate subgoals that steer the system into more favorable regimes.

To generate sequential behavior as in [13], we simply execute the steepest gradient at every time step (Eq. (2), where \mathbf{k} is a control gain). This ensures robust progress even when some paths stall at local stationary points.

$$\mathbf{a}_{t+1} = \mathbf{a}_t - \mathbf{k} \cdot \nabla_{\mathbf{a}}^{p^*} g \quad p^* = \operatorname{argmax}_{p \in \mathbb{P}} \|\nabla_{\mathbf{a}}^p g\| \quad (2)$$

This mechanism allows AICON to jointly perform perception and action selection for sequential, feedback-driven behavior [13]. However, it cannot cope with conflicting goals and their gradients. To address this limitation, we leverage the same gradient structure but replace the steepest-selection rule (Eq. (2)) with a combination of gradients through their nullspaces, as described next.

B. Nullspace Projections for Conflict Resolution

When the gradients along multiple paths are simultaneously relevant, they might interfere, leading to conflicting updates in action space. A common strategy to mitigate this is to project the lower-priority gradient onto the subspace that does not conflict with the higher-priority one—its nullspace.

Formally, given a gradient $\nabla_{\mathbf{q}}^{p_1} g$ along path p_1 that relates a quantity \mathbf{q} to a goal's error signal, we define a projection operator \mathcal{N}_1 that removes interfering components of the gradient $\nabla_{\mathbf{q}}^{p_2} g$ along a second path p_2 . This yields a conflict-free combined gradient:

$$\nabla_{\mathbf{q}}^{p_1 \triangleright p_2} g = \nabla_{\mathbf{q}}^{p_1} g + \mathcal{N}_1 \nabla_{\mathbf{q}}^{p_2} g. \quad (3)$$

In the general nullspace formulation, this projector \mathcal{N}_1 is computed using the pseudoinverse $\mathbf{J}_1^\#$ of the respective Jacobian (Eq. (4)) along p_1 . However, this approach is computationally expensive and numerically unstable. In practice, more efficient formulations based on QR decomposition (Eq. (5)) are often used to avoid inversion.

In AICON (as in many optimization settings), all goals are scalar cost functions. This allows us to simplify the projector further to an orthogonalization step. Under this assumption, the projector can be obtained simply from the normalized gradient. The resulting projector ensures non-interference while remaining computationally efficient:

$$\mathcal{N}_1 = \mathbf{I} - \mathbf{J}_1^\# \mathbf{J}_1 \quad (4)$$

$$= \mathbf{I} - \mathbf{Q}_1 \mathbf{Q}_1^T \quad \text{using } \mathbf{J}_1^T = \mathbf{Q}_1 \mathbf{R}_1 \quad (5)$$

$$= \mathbf{I} - \mathbf{v}_1 \mathbf{v}_1^T \quad \text{using } \mathbf{Q}_1 = \mathbf{v}_1 = \nabla_{\mathbf{q}}^{p_1} g / \|\nabla_{\mathbf{q}}^{p_1} g\|. \quad (6)$$

While the projector itself follows from standard nullspace control [15], its application here differs in three key ways: goals are scalar cost functions, enabling the efficient orthogonalization in Eq. (6) without pseudoinverse computation; projections occur at intermediate representations throughout the graph rather than only at the final action space; and crucially, the priority ordering is not fixed in advance but determined continuously from the current gradient magnitudes,

as described next. This last point is what allows conflict resolution to adapt as the state evolves, rather than reflecting a hand-engineered hierarchy.

C. Continuously Resolving Goal Conflicts and Preventing Local Minima

While projecting one gradient orthogonal to another (Eqs. (3) and (6)) prevents direct interference, AICON leverages this mechanism across multiple interconnected components (Eq. (1)) to resolve conflicts more broadly. At each state space along the path, gradients can be projected onto one another, yielding a layered resolution process: gradients of progressively lower-priority goals are projected into the orthogonal complements of higher-priority ones wherever they begin to overlap. This continuous resolution of conflicts enables many concurrent goals to be accommodated robustly.

Since gradient magnitude reflects both local sensitivity and the system's current ability to reduce a given cost, they allow us to determine priorities dynamically. At every quantity \mathbf{q} , we select the steepest gradient in the remaining space as long as degrees of freedom remain, i.e., we first select the gradient with the largest magnitude, analogously to the single-goal case (Eq. (2)), then each subsequent gradient according to its magnitude after projection against all previously selected gradients:

$$\nabla_{\mathbf{q}}^{[i]} g = \operatorname{argmax}_{\nabla g \in \mathbb{G}_{\mathbf{q}}^{[i]}} \|\nabla g\|, \quad (7)$$

$$\mathbb{G}_{\mathbf{q}}^{[i]} = \left\{ \left[\prod_{k=1}^{i-1} \mathcal{N}_{[k]} \right] \nabla g \mid \nabla g \in \mathbb{G}_{\mathbf{q}}^{[0]} \setminus \{ \nabla_{\mathbf{q}}^{[j]} g \}_{j=1}^{i-1} \right\}. \quad (8)$$

Here, $\mathbb{G}_{\mathbf{q}}^{[0]}$ is the set of all candidate gradients for quantity \mathbf{q} , $\mathbb{G}_{\mathbf{q}}^{[i]}$ the remaining candidates after $i-1$ projections, $\nabla_{\mathbf{q}}^{[i]} g$ the i -th selected gradient in descending priority, and $\mathcal{N}_{[i]}$ its associated projector (Eq. (6)). The resulting gradients are orthogonal, so their sum produces a conflict-free gradient for the next quantity on the path.

Importantly, the notion of a "goal" is not restricted to explicitly defined cost functions: every gradient propagating through the network—whether from distinct cost functions or different paths of the same one—is treated uniformly. Projections can occur at any intermediate representation along the propagation paths wherever gradients begin to overlap. This projection-aware ordering mechanism for conflict resolution allows AICON to integrate diverse influences flexibly and robustly without explicit hierarchies or manual arbitration.

D. Escaping Local Minima

While the described projection mechanism resolves many conflicts in a way that prevents local minima from forming, some problems induce conflicts that no linear combination of gradients can resolve. A classic case is 2D navigation with non-convex obstacles: if the target lies behind an obstacle, the goal and avoidance gradients may point in opposite directions, trapping descent in a local minimum. Beyond anticipation-based solutions [8,31], a simple heuristic in this case is wall-following [27,28]: instead of moving toward or

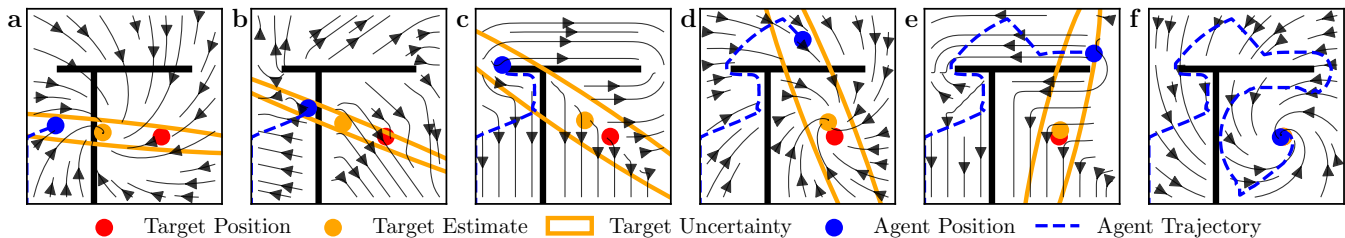


Fig. 1. Adaptive conflict resolution solves 2D navigation in a non-convex obstacle configuration that static potential fields cannot solve. To visualize the evolving potential (background, arrows), we densely sample the gradient across the space given the current projections—note that only the local gradient is computed during execution. The composite potential field evolves continuously as gradients are projected into one another’s nullspaces. (a) The agent (blue) moves toward the target (red), reducing positional uncertainty (orange ellipse around target estimate, orange dot) by triangulating in the nullspace of the goal gradient. (b) Attractive and repulsive gradients begin to oppose each other as the agent approaches the obstacle, potentially forming a local minimum. (c–e) Nullspace explorations move the agent along the obstacle boundary until the conflict weakens and a viable path opens. (f) Normal goal pursuit resumes and the agent reaches the target.

away from the obstacle, the agent progresses along its boundary until a path opens. We can reinterpret this as exploration in the obstacle’s nullspace, where motion orthogonal to the avoidance gradient eventually resolves the conflict.

We generalize this idea in AICON. A conflict is detected when the two strongest gradients have a cosine similarity below a threshold $\theta_{\text{enter}} = -0.6$, indicating near-opposition. Upon detection, the system enters exploration mode: it moves along the direction within the nullspace of the dominant gradient that is most consistent with recent motion history, represented as an exponential moving average of the corresponding quantity. This breaks directional symmetry and prevents oscillation by biasing continuation over reversal. Exploration terminates when the cosine similarity rises above $\theta_{\text{exit}} = -0.4$ or one gradient exceeds all others in magnitude by a factor $\lambda = 3$, at which point normal goal pursuit resumes. The asymmetric thresholds provide hysteresis, preventing rapid re-entry into exploration. Since gradients propagate through many interconnected components, this detection-resolution cycle can occur at any intermediate representation along the propagation paths, flexibly leveraging the full structure of the system for conflict resolution.

E. Stabilizing the Control Signal

Since priorities are determined dynamically based on projected gradient magnitudes (Eq. (7)), small changes in the system state can lead to discrete changes in the ordering. These switches introduce discontinuities in the resulting control signal and may cause oscillatory behavior.

To mitigate this effect, we introduce hysteresis in the priority selection: a change in ordering is only accepted if a competing gradient exceeds the current one by a margin of 10%. This prevents rapid switching when gradients are of similar magnitude. Additionally, we apply temporal smoothing to the resulting control signal using a low-pass filter, further reducing high-frequency oscillations. Moreover, the escape mechanism described in Sect. III-D incorporates asymmetric thresholds for entering and leaving exploration, providing an additional source of hysteresis.

A second source of instability arises from the dependence of gradient magnitudes on the parametrization of cost functions and the structure of the system. Since priorities are

based on these magnitudes, inconsistent scaling can lead to undesirable orderings. To address this, we normalize gradient magnitudes before projection using a softmax with temperature $\tau = 0.8$. This effectively decouples the qualitative structure of priorities—which gradients should dominate in which situations—from their precise quantitative scaling, since softmax preserves relative ordering while compressing absolute differences. As a result, system design can focus on ensuring correct priority relationships across situations rather than careful magnitude tuning, improving robustness to reparametrization of individual cost functions.

The parameters governing transition sharpness and hysteresis width— θ_{enter} , θ_{exit} , λ , the priority hysteresis margin, and the softmax temperature τ —do not require careful tuning. For θ_{enter} and θ_{exit} , the asymmetry between them matters more than their absolute values, controlling hysteresis width and preventing chattering. λ sets the magnitude ratio at which a dominant gradient cleanly terminates exploration, τ shapes how sharply the softmax distinguishes priority levels, and the priority margin prevents rapid reordering when gradients are of similar magnitude. We verified across the one-hundred *pushT* configurations that success rate is preserved across reasonable variations of each, with trajectories and completion times varying but qualitative behavior remaining intact—reflecting that these parameters govern the sharpness and timing of transitions rather than the underlying conflict resolution mechanism.

IV. CONFLICT RESOLUTION IN 2D NAVIGATION

Navigation in cluttered environments is a canonical testbed for studying multi-objective conflicts in robotics. Classical potential field methods often fail in these settings: non-convex obstacles induce local minima where the attractive gradient to the goal directly opposes repulsive gradients from obstacles, requiring either precomputed planning [8,31] or heuristic strategies such as wall-following [27].

We use this task to highlight the power of AICON’s adaptive conflict resolution. When obstacles introduce conflicting gradients, nullspace projection and exploration enable the agent to explore alternative directions, escaping local minima. This produces fully reactive behavior that successfully resolves multi-objective conflicts, demonstrating that local

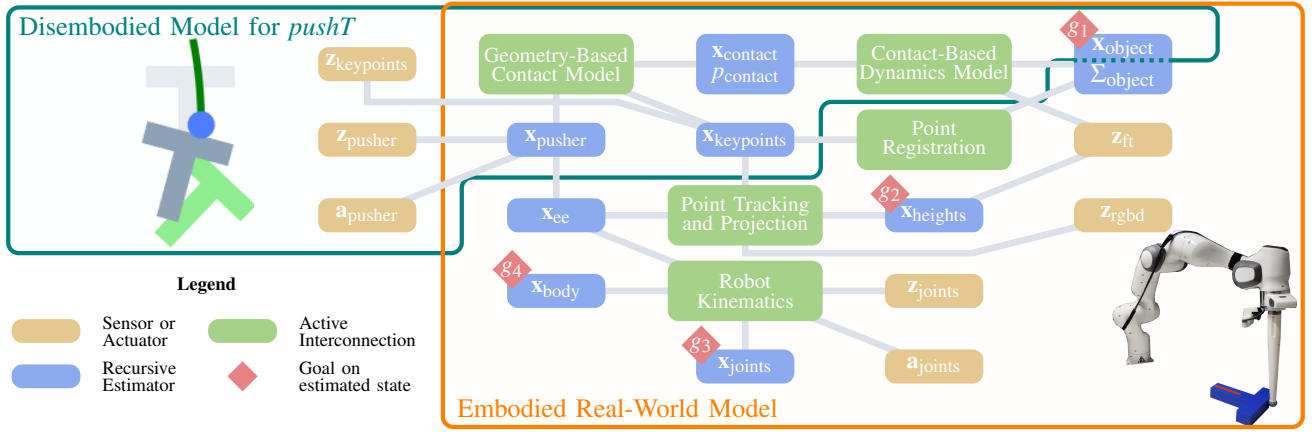


Fig. 2. By coupling state estimators through active interconnections, we construct a model that solves the pushT task through reactive gradient-based control (green box). When interconnected with additional estimators into a larger model (orange box), the same approach solves object pushing on a real robot. The real-world model introduces additional goals, including perceptual uncertainty reduction and joint limit avoidance, that our approach seamlessly incorporates through the same conflict resolution mechanism.

minima are a consequence of static encodings rather than inherent task complexity (Fig. 1).

Model: We simulate a 2D agent with planar position $\mathbf{x}_{\text{rob}} \in \mathbb{R}^2$ and velocity control $\mathbf{a} \in \mathbb{R}^2$. The agent receives bearing-only measurements to the target $\mathbf{z}_{\text{tar}} \in \mathbb{R}^1$ and range measurements to the nearest obstacle $\mathbf{z}_{\text{obs}} \in \mathbb{R}^1$.

AICON encodes three internal estimates: the agent’s position \mathbf{x}_{rob} , the current distance to the closest obstacle \mathbf{x}_{obs} , and a Gaussian belief over the location of the target $\mathbf{x}_{\text{tar}} \sim \mathcal{N}(\boldsymbol{\mu}_{\text{tar}}, \boldsymbol{\Sigma}_{\text{tar}})$ relative to the agent. These are coupled through simple active interconnections that propagate information between actuation signals and state variables.

Goals and Gradients: The primary objective is minimizing the expected distance to the goal while avoiding collisions with obstacles. We define scalar cost functions on the relative target location and the distance to obstacles:

$$g_1 = \mathbb{E}[\|\mathbf{x}_{\text{tar}}\|] = \|\boldsymbol{\mu}_{\text{tar}}\| + \text{Tr}(\boldsymbol{\Sigma}_{\text{tar}}), \quad g_2 = p_{\text{collision}}(\mathbf{x}_{\text{obs}}).$$

where $p_{\text{collision}}$ is the likelihood of collision, decreasing with distance and representing a repulsive potential for obstacles. Gradients of these costs are propagated through AICON’s interconnections to the actuation signals, leading to three distinct gradient paths that reduce distance to the target (p_1), uncertainty over the target distance (p_2), and likelihood of collision (p_3):

$$\nabla_{\mathbf{a}}^{p_1} g_1 = \frac{\partial g_1}{\partial \boldsymbol{\mu}_{\text{tar}}} \frac{\partial \boldsymbol{\mu}_{\text{tar}}}{\partial \mathbf{x}_{\text{rob}}} \frac{\partial \mathbf{x}_{\text{rob}}}{\partial \mathbf{a}}, \quad \nabla_{\mathbf{a}}^{p_2} g_1 = \frac{\partial g_1}{\partial \boldsymbol{\Sigma}_{\text{tar}}} \frac{\partial \boldsymbol{\Sigma}_{\text{tar}}}{\partial \mathbf{x}_{\text{rob}}} \frac{\partial \mathbf{x}_{\text{rob}}}{\partial \mathbf{a}},$$

$$\nabla_{\mathbf{a}}^{p_3} g_2 = \frac{\partial g_2}{\partial \mathbf{x}_{\text{obs}}} \frac{\partial \mathbf{x}_{\text{obs}}}{\partial \mathbf{x}_{\text{rob}}} \frac{\partial \mathbf{x}_{\text{rob}}}{\partial \mathbf{a}}.$$

Qualitative Behavior: Behavior emerges as a sequence of continuous adjustments rather than preplanned trajectories, as shown in Fig. 1. Initially, the agent moves toward the goal while reducing positional uncertainty through emergent triangulation in the nullspace of the goal gradient (\mathbf{a}). As it approaches non-convex obstacle boundaries, attractive and repulsive gradients begin to oppose each other (\mathbf{b}), triggering

nullspace exploration along the obstacle boundary until a viable path opens (\mathbf{c} – \mathbf{e}). Normal goal pursuit then resumes and the agent reaches the target (\mathbf{f}).

V. CONFLICT RESOLUTION IN OBJECT PUSHING

Object pushing provides a natural testbed for our thesis, since multiple, competing objectives—beneficial contacts to pursue, detrimental contacts to avoid, and perceptual or kinematic constraints—interact to create local minima, which must be resolved online without explicit planning. Non-convex objects in particular lead to problems: the gradient of a target contact may directly oppose that of a contact that must be avoided, as in the widely used *pushT* task [17] where a T-shaped object must be pushed into a target pose. Using only an approximate dynamics model, AICON resolves these conflicts and successfully completes the task from arbitrary start-goal configurations (Sect. V-A).

To further challenge the approach, we embed the same model into one that reflects the embodiment and perception constraints of a real-world pushing setup, introducing additional goals such as reducing perceptual uncertainty and respecting kinematic limits. Without modifying the contact-based dynamics model, our approach transfers directly, with the continuous conflict-resolution accommodating these additional constraints and objectives (Sect. V-B).

A. *pushT*: Object Pushing in Simulation

The *pushT* task, in which a T-shaped object must be pushed into a target pose in a 2D environment (Fig. 2, green model), has become a standard benchmark, in particular in imitation learning [17]. Here, we use it, because its non-convex geometry induces structural local minima: if the robot approaches from the wrong side, all immediately available contacts move the object further from the goal, requiring the robot to retreat, move around the object, and approach from another direction.



Fig. 3. Representative rollout of AICON on the pushT task. (a) The robot (blue) positions itself to increase contact likelihood with the T-shaped object (gray) while modulating contact position in the nullspace. (b) Model imprecision causes the object to be pushed too far without sufficient rotation; the robot reduces contact likelihood to avoid compounding the error. (c) Useful contacts now lie only on the opposite side, creating directly opposing gradients; the system enters nullspace exploration rather than stalling. (d) The robot navigates to the far side of the object. (e) A second conflict arises at a corner contact and is resolved through a brief additional exploration phase. (f) The robot pushes the object into the target pose (green).

Model: We model pushT in AICON using a minimal set of observations and actions: the pusher’s 2D location $\mathbf{z}_{\text{pusher}} \in \mathbb{R}^2$, the object’s N corner keypoints $\mathbf{z}_{\text{keypoints}} \in \mathbb{R}^{N \times 2}$, and the pusher’s velocity as actuation signal $\mathbf{a}_{\text{pusher}} \in \mathbb{R}^2$. From these, we estimate the pusher position $\mathbf{x}_{\text{pusher}}$, object keypoints $\mathbf{x}_{\text{keypoints}}$, and the object pose \mathbf{x}_{obj} (centroid and orientation). Possible contacts $\mathbf{x}_{\text{contact}} \in \mathbb{R}^{N \times 2}$ are defined as the closest points on each of the N object sides, with likelihoods p_{contact} decreasing with distance (geometry-based contact model in Fig. 2). Object motion under contact is approximated by translation along the contact normal, combined with rotation proportional to the angle between the normal and the vector from contact to centroid. The net effect is a likelihood-weighted combination of all possible contacts (contact-based dynamics model in Fig. 2). Compared to analytic [16,32] or data-driven [33] models, ours is deliberately coarse: it does not aim for accurate object-specific dynamics, but captures generic pushing regularities, enabling transfer across objects and environments.

Goal and Gradients: The task goal is defined as minimizing object-target pose error, $g_1 = \|\mathbf{x}_{\text{obj}} - \mathbf{x}_{\text{target}}\|$. This yields two gradient paths per contact: one through its likelihood (p_1) and one through its position (p_2):

$$\nabla_{\mathbf{a}_{\text{pusher}}}^{p_1} g_1 = \frac{\partial g_1}{\partial \mathbf{x}_{\text{obj}}} \frac{\partial \mathbf{x}_{\text{obj}}}{\partial p_{\text{contact}}} \frac{\partial p_{\text{contact}}}{\partial \mathbf{x}_{\text{pusher}}} \frac{\partial \mathbf{x}_{\text{pusher}}}{\partial \mathbf{a}_{\text{pusher}}},$$

$$\nabla_{\mathbf{a}_{\text{pusher}}}^{p_2} g_1 = \frac{\partial g_1}{\partial \mathbf{x}_{\text{obj}}} \frac{\partial \mathbf{x}_{\text{obj}}}{\partial \mathbf{x}_{\text{contact}}} \frac{\partial \mathbf{x}_{\text{contact}}}{\partial \mathbf{x}_{\text{pusher}}} \frac{\partial \mathbf{x}_{\text{pusher}}}{\partial \mathbf{a}_{\text{pusher}}}.$$

Qualitative Behavior: With these gradients, the projection mechanism (Sect. III-C), and local-minima escape (Sect. III-D), AICON generates successful behaviors in pushT. A representative rollout is shown in Fig. 3: the robot first positions itself to make contact while resolving the position-likelihood conflict in the nullspace (a–b), then navigates around the object when useful contacts lie only on the opposite side (c–d), resolves a second conflict at a corner (e), and finally pushes the object into the target pose (f).

Quantitative Results: Across one-hundred randomly generated start-goal configurations, AICON leveraging nullspaces consistently resolves conflicts and avoids local minima (Fig. 4). The steepest-descent baseline from [13]—which selects the single strongest gradient at each step without projection or conflict resolution—achieves 0% success, with all failures arising from local minima at structural conflict points. This directly quantifies the contribution of

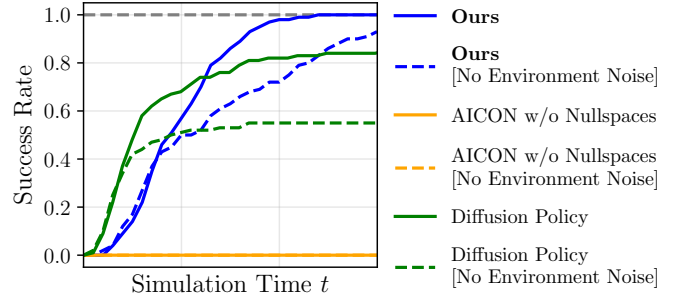


Fig. 4. Success rate over time across one-hundred randomized robot-object configurations. AICON (blue) reaches 100% success under realistic action noise (solid) and 95% in the fully deterministic setting (dashed), with the remaining 5% entering long limit cycles rather than failing to escape local minima. AICON without nullspace exploitation (yellow) stalls at structural conflict points for all configurations, directly quantifying the contribution of adaptive conflict resolution. Diffusion policy (green) plateaus at approximately 55% in the deterministic setting (dashed), showing how configurations outside the training distribution induce failures analogous to local minima; with additional action noise (solid), it recovers up to 85%.

adaptive conflict resolution over myopic gradient following. A pixel-based diffusion policy [17] reaches approximately 55% in the deterministic setting, with failures reflecting brittleness to configurations outside the training distribution. These configurations lead to stalling progress analogous to local minima. With action noise, it recovers to 85%, while AICON reaches 100%, with the remaining 5% failures for the purely deterministic setting arising from limit cycles rather than inability to escape local minima. We additionally verified that AICON’s performance is invariant to absolute goal pose and actuation speed constraints, as expected from its goal-agnostic conflict resolution, whereas diffusion policy degrades significantly under these variations.

In the following, we show that the same model transfers directly to real-world pushing, where additional perceptual and kinematic goals introduce further conflicts.

B. Real-World Transfer: Handling Additional Goal Conflicts

We now transfer the model from 2D simulation to a real robot with only on-board sensing (Fig. 2, orange model). The model itself is unchanged apart from unit scaling; the difference lies in replacing idealized sensing and actuation with an in-hand RGBD camera, a force-torque sensor, and joint-level proprioception and control. These substitutions require additional estimators, active interconnections, and introduce new goals that may conflict with the main objective,

providing a strong testbed for AICON’s conflict resolution.

Model: We conduct our experiments on a Panda robot equipped with a custom pusher, an in-hand RGBD camera, and a force-torque sensor. Proprioception $\mathbf{z}_{\text{joints}}$ and actuation $\mathbf{a}_{\text{joints}}$ yield joint states $\mathbf{x}_{\text{joints}}$, from which the kinematics provide the end-effector pose \mathbf{x}_{ee} relevant for the position of the push-stick and the body frames \mathbf{x}_{body} for self-collision checks. The camera provides segmented object keypoints $\mathbf{z}_{\text{keypoints}}$ and a reference marker for the object’s orientation. Depth values allow estimation of the relative height difference $\mathbf{x}_{\text{heights}}$ between pusher and object and a pose uncertainty Σ_{obj} , which grows when the object lies near the image border. Force-torque signals \mathbf{z}_{ft} further inform contact likelihoods and relative height.

Goals and Gradients: The task goal remains minimizing object-target error, now extended to penalize perceptual uncertainty: $g_1 = \|\mathbf{x}_{\text{obj}} - \mathbf{x}_{\text{target}}\| + \text{Tr}(\Sigma_{\text{obj}})$. This produces gradients not only for pushing but also for adjusting the camera viewpoint. Additional goals include maintaining contact height ($g_2 = \|\mathbf{x}_{\text{heights}}\|$), avoiding joint limits ($g_3 = p_{\text{limit}}(\mathbf{x}_{\text{joints}})$), and preventing self-collisions ($g_4 = p_{\text{collision}}(\mathbf{x}_{\text{body}})$). Each propagates straightforwardly through the kinematics to the joint space.

Qualitative Behavior: Overall, the pushing behavior remains similar to simulation, but new conflicts arise from perception and robot constraints. Ambiguities in keypoint tracking and deviations from the coarse contact model often lead to errors, e.g., bumping a corner, yet AICON recovers and still drives the object to the target.

The added goals generate distinctive behaviors: uncertainty reduction encourages the robot to lift and center the object in view, counteracted by the height-maintenance goal, leading sometimes to small vertical oscillations. The camera is continuously reoriented toward the object, reflecting active perception. Joint limits and self-collisions rarely dominate, but when approached, the robot redirects into free directions rather than stalling. Situations requiring nullspace exploration (Sect. III-D) primarily arise from the 2D pushing dynamics, with only rare interference from other goals, e.g., camera reorientation near a joint limit.

These results show that the projection mechanism seamlessly accommodates additional real-world conflicts without altering the underlying object dynamics model. Moreover, they demonstrate that the conflict resolution generalizes from simulation to real robots, supporting our thesis that online negotiation between objectives can replace planning in complex, multi-objective tasks.

VI. DISCUSSION

Solvable Problem Classes and Limitations: Conflict resolution via nullspaces broadens the class of solvable problems of AICON beyond compatible subgoals, allowing concurrent conflicts to be resolved—given sufficient time. This reveals both the strengths and limits of the approach. Local, simultaneous conflicts can be resolved reactively, but conflicts that only emerge through long-term interactions (e.g., Tower of

Hanoi, where an early wrong move blocks later progress) remain practically unsolvable. Importantly, the method ensures eventual progress rather than optimality, akin to probabilistic completeness: a solution is likely to be found if it exists, though not necessarily efficiently.

This solvable problem class mirrors early work on the hierarchy of planning difficulties. Conflict-free or nearly serializable tasks are easiest [12], while tasks with mostly invalid sequences or those requiring undoing prior subgoals remain hard [11,12]. Following Moravec’s paradox, however, the relevant conflicts of most robotic manipulation are not of these pathological kinds, but instead arise between simultaneously relevant goals, where robustness of behavior is typically more important than exact optimality.

Connections to Learning and Optimization Approaches: Conflicting objectives also arise in learning and optimization, where they can trap progress in local minima [34]. Multi-objective methods often mitigate this by adjusting updates based on gradient relationships [35]–[37], since simple linear combinations rarely suffice [34]. Our results suggest a complementary path: rather than only reshaping update rules, explicitly dynamizing the optimization landscape could improve robustness. In our approach, the landscape shifts continuously as priorities change, new gradient paths become dominant, and connected states evolve, making the effective optimization surface non-stationary by design. Even the constructive role of action noise observed in our pushT results, where deterministic execution produces limit cycles that stochasticity resolves, can be understood in this light: noise perturbs the effective landscape, breaking periodicity that the gradient-based dynamics alone cannot escape. This parallels the role of noise in SGD [38], but generalizes it: non-stationarity arises not only from injected randomness but from the structure of the problem itself. This suggests framing landscape non-stationarity not as a problem to be avoided but as a general mechanism for escaping unproductive dynamics—one that optimization methods could exploit more deliberately.

Connections to Biological Control and Decision-Making: As previously argued in [13], AICON already shares structural and behavioral similarities with biological systems, making it suitable for modeling biological behavior [39]–[42]. Nullspace projection strengthens this connection, reflecting principles from motor control and decision-making. In human motor control, task-relevant dimensions are stabilized while null dimensions remain free and can be exploited to accommodate secondary objectives [43]–[46]. These free dimensions are also explored during learning [47]. Neural population studies show that adaptive computations in nullspaces support projection-based control, both in motor systems [48]–[50] and in higher-level decision-making in the prefrontal cortex [51]–[53]. These parallels suggest that projection into nullspaces is not only computationally effective but also biologically plausible, making it a particularly promising principle for adaptive real-world behavior.

VII. CONCLUSION

We showed that a broad class of multi-objective behaviors typically addressed through planning can instead be generated reactively, by resolving conflicts between simultaneously active objectives through adaptive nullspace projections. The extended AICON framework handles tasks previously intractable for reactive methods, transfers from simulation to real robots without modification, and accommodates additional constraints through the same mechanism—suggesting that the boundary between planning and control reflects the limitations of static objective representations more than the inherent structure of the tasks themselves.

REFERENCES

- [1] R. E. Fikes and N. J. Nilsson, “STRIPS: A new approach to the application of theorem proving to problem solving,” *Artificial Intelligence*, vol. 2, no. 3-4, pp. 189–208, 1971.
- [2] C. R. Garrett, R. Chitnis, R. Holladay, B. Kim, T. Silver, L. P. Kaelbling, and T. Lozano-Pérez, “Integrated task and motion planning,” *Annual Review of Control, Robotics, and Autonomous Systems*, vol. 4, no. 1, pp. 265–293, 2021.
- [3] M. Toussaint, J.-S. Ha, and D. Driess, “Describing physics for physical reasoning: Force-based sequential manipulation planning,” *Robotics and Automation Letters*, vol. 5, no. 4, pp. 6209–6216, 2020.
- [4] R. Brooks, “A robust layered control system for a mobile robot,” *Journal on Robotics and Automation*, vol. 2, no. 1, pp. 14–23, 1986.
- [5] O. Khatib, “A unified approach for motion and force control of robot manipulators: The operational space formulation,” *Journal of Robotics and Automation*, vol. 3, no. 1, pp. 43–53, 1987.
- [6] E. Gat, R. P. Bonnasso, R. Murphy *et al.*, “On three-layer architectures,” *Artificial Intelligence and Mobile Robots*, vol. 195, art. no. 210, 1998.
- [7] D. E. Koditschek and E. Rimon, “Robot navigation functions on manifolds with boundary,” *Advances in Applied Mathematics*, vol. 11, no. 4, pp. 412–442, 1990.
- [8] E. Rimon and D. Koditschek, “Exact robot navigation using artificial potential functions,” *Transactions on Robotics and Automation*, vol. 8, no. 5, pp. 501–518, 1992.
- [9] J. P. Lewis and M. Weir, “Subgoal chaining and the local minimum problem,” *International Joint Conference on Neural Networks*, pp. 1844–1849, 1999.
- [10] A. Colotti, J. G. Fontán, A. Goldsztejn, S. Briot, F. Chaumette, O. Kermorgant, and M. S. E. Din, “Determination of all stable and unstable equilibria for image-point-based visual servoing,” *Transactions on Robotics*, vol. 40, pp. 3406–3424, 2024.
- [11] R. E. Korf, “Planning as search: A quantitative approach,” *Artificial Intelligence*, vol. 33, no. 1, pp. 65–88, 1987.
- [12] A. Barret and D. Weld, “Characterizing subgoal interactions for planning,” *International Joint Conference on Artificial Intelligence*, pp. 1388–1393, 1993.
- [13] V. Mengers and O. Brock, “No plan but everything under control: Robustly solving sequential tasks with dynamically composed gradient descent,” *International Conference on Robotics and Automation*, pp. 90–96, 2025.
- [14] R. Martín-Martín and O. Brock, “Coupled recursive estimation for online interactive perception of articulated objects,” *The International Journal of Robotics Research*, vol. 41, no. 8, pp. 741–777, 2019.
- [15] A. Dietrich, C. Ott, and A. Albu-Schäffer, “An overview of null space projections for redundant, torque-controlled robots,” *The International Journal of Robotics Research*, vol. 34, no. 11, pp. 1385–1400, 2015.
- [16] P. Perugini, J. Lundell, K. Friedl, and D. Kragic, “Pushing everything everywhere all at once: Probabilistic prehensile pushing,” *Robotics and Automation Letters*, vol. 10, no. 5, pp. 4540–4547, 2025.
- [17] C. Chi, Z. Xu, S. Feng, E. Cousineau, Y. Du, B. Burchfiel, R. Tedrake, and S. Song, “Diffusion policy: Visuomotor policy learning via action diffusion,” *The International Journal of Robotics Research*, vol. 44, no. 10-11, pp. 1684–1704, 2025.
- [18] Z. Jiao, Y. Niu, Z. Zhang, S.-C. Zhu, Y. Zhu, and H. Liu, “Sequential manipulation planning on scene graph,” *International Conference on Intelligent Robots and Systems*, pp. 8203–8210, 2022.
- [19] M. Posa, C. Cantu, and R. Tedrake, “A direct method for trajectory optimization of rigid bodies through contact,” *The International Journal of Robotics Research*, vol. 33, no. 1, pp. 69–81, 2014.
- [20] Y. Zhang, T. Xue, A. Razmjoo, and S. Calinon, “Learning problem decomposition for efficient sequential multi-object manipulation planning,” *Robotics and Automation Letters*, vol. 10, no. 12, pp. 13367–13374, 2025.
- [21] A. Brohan, Y. Chebotar, C. Finn, K. Hausman, A. Herzog, D. Ho, J. Ibarz, A. Irpan, E. Jang, R. Julian *et al.*, “Do as i can, not as i say: Grounding language in robotic affordances,” *Conference on Robot Learning*, pp. 287–318, 2023.
- [22] D. Driess, F. Xia, M. S. M. Sajjadi, C. Lynch, A. Chowdhery, B. Ichter, A. Wahid, J. Tompson, Q. Vuong, T. Yu, W. Huang, Y. Chebotar, P. Sermanet, D. Duckworth, S. Levine, V. Vanhoucke, K. Hausman, M. Toussaint, K. Greff, A. Zeng, I. Mordatch, and P. Florence, “PaLM-E: an embodied multimodal language model,” *International Conference on Machine Learning*, art. no. 340, 2023.
- [23] D. Kalashnikov, A. Irpan, P. Pastor, J. Ibarz, A. Herzog, E. Jang, D. Quillen, E. Holly, M. Kalakrishnan, V. Vanhoucke *et al.*, “Scalable deep reinforcement learning for vision-based robotic manipulation,” *Conference on Robot Learning*, pp. 651–673, 2018.
- [24] G. Dulac-Arnold, N. Levine, D. J. Mankowitz, J. Li, C. Paduraru, S. Gowal, and T. Hester, “Challenges of real-world reinforcement learning: definitions, benchmarks and analysis,” *Machine Learning*, vol. 110, no. 9, pp. 2419–2468, 2021.
- [25] C. He, X. Liu, G. S. Camps, G. Sartoretti, and M. Schwager, “Demystifying diffusion policies: Action memorization and simple lookup table alternatives,” *Preprint arXiv:2505.05787*, 2025.
- [26] D. Ghosh, J. Rahme, A. Kumar, A. Zhang, R. P. Adams, and S. Levine, “Why generalization in RL is difficult: Epistemic POMDPs and implicit partial observability,” *Advances in Neural Information Processing Systems*, vol. 34, pp. 25502–25515, 2021.
- [27] P. Van Turrenout, G. Honderd, and L. Van Schelven, “Wall-following control of a mobile robot,” *International Conference on Robotics and Automation*, pp. 280–285, 1992.
- [28] X. Yun and K.-C. Tan, “A wall-following method for escaping local minima in potential field based motion planning,” *International Conference on Advanced Robotics*, pp. 421–426, 1997.
- [29] M. Iovino, J. Förster, P. Falco, J. J. Chung, R. Siegwart, and C. Smith, “Comparison between behavior trees and finite state machines,” *Transactions on Automation Science and Engineering*, vol. 22, pp. 21098–21117, 2025.
- [30] N. D. Ratliff, J. Issac, D. Kappler, S. Birchfield, and D. Fox, “Riemannian motion policies,” *Preprint arXiv:1801.02854*, 2018.
- [31] L. E. Kavraki, P. Svestka, J.-C. Latombe, and M. H. Overmars, “Probabilistic roadmaps for path planning in high-dimensional configuration spaces,” *Transactions on Robotics and Automation*, vol. 12, no. 4, pp. 566–580, 2002.
- [32] M. T. Mason, “Mechanics and planning of manipulator pushing operations,” *The International Journal of Robotics Research*, vol. 5, no. 3, pp. 53–71, 1986.
- [33] M. Bauza, F. R. Hogan, and A. Rodriguez, “A data-efficient approach to precise and controlled pushing,” *Conference on Robot Learning*, pp. 336–345, 2018.
- [34] Y. Hu, R. Xian, Q. Wu, Q. Fan, L. Yin, and H. Zhao, “Revisiting scalarization in multi-task learning: A theoretical perspective,” *Neural Information Processing Systems*, pp. 48510–48533, 2023.
- [35] B. Liu, X. Liu, X. Jin, P. Stone, and Q. Liu, “Conflict-averse gradient descent for multi-task learning,” *Neural Information Processing Systems*, pp. 18878–18890, 2021.
- [36] S. Liu, S. James, A. J. Davison, and E. Johns, “Auto-lambda: Disentangling dynamic task relationships,” *Transactions on Machine Learning Research*, 2022.
- [37] S. Zhou, W. Zhang, J. Jiang, W. Zhong, J. Gu, and W. Zhu, “On the convergence of stochastic multi-objective gradient manipulation and beyond,” *Neural Information Processing Systems*, pp. 38103–38115, 2022.
- [38] R. Kleinberg, Y. Li, and Y. Yuan, “An alternative view: When does SGD escape local minima?” *International Conference on Machine Learning*, pp. 2698–2707, 2018.
- [39] V. Mengers, M. Raoufi, O. Brock, H. Hamann, and P. Romanczuk, “Leveraging uncertainty in collective opinion dynamics with heterogeneity,” *Scientific Reports*, vol. 14, art. no. 27314, 2024.
- [40] A. Battaja, A. Godinez, N. M. Hanning, M. Rolfes, and O. Brock, “An

information processing pattern from robotics predicts properties of the human visual system,” *Preprint bioRxiv:2024.06.20.599814*, 2024.

- [41] V. Mengers, N. Roth, O. Brock, K. Obermayer, and M. Rolf, “A robotics-inspired scanpath model reveals the importance of uncertainty and semantic object cues for gaze guidance in dynamic scenes,” *Journal of Vision*, vol. 25, no. 2, art. no. 6, 2025.
- [42] M. Migacev, V. Mengers, A. Köngeter, and O. Brock, “No plan, yet human: A reactive robotics model predicts human planning failures on a clinical task,” *Preprint arXiv:2605.16514*, 2026.
- [43] J. P. Scholz and G. Schöner, “The uncontrolled manifold concept: identifying control variables for a functional task,” *Experimental Brain Research*, vol. 126, no. 3, pp. 289–306, 1999.
- [44] M. L. Latash, J. P. Scholz, and G. Schöner, “Motor control strategies revealed in the structure of motor variability,” *Exercise and Sport Sciences Reviews*, vol. 30, no. 1, pp. 26–31, 2002.
- [45] A. d. Ruyg, G. E. Loeb, and T. J. Carroll, “Muscle coordination is habitual rather than optimal,” *Journal of Neuroscience*, vol. 32, no. 21, pp. 7384–7391, 2012.
- [46] D. Furuki and K. Takiyama, “Decomposing motion that changes over time into task-relevant and task-irrelevant components in a data-driven manner: application to motor adaptation in whole-body movements,” *Scientific Reports*, vol. 9, no. 1, art. no. 7246, 2019.
- [47] P. Singh, S. Jana, A. Ghosal, and A. Murthy, “Exploration of joint redundancy but not task space variability facilitates supervised motor learning,” *Proceedings of the National Academy of Sciences*, vol. 113, no. 50, pp. 14414–14419, 2016.
- [48] M. M. Churchland, J. P. Cunningham, M. T. Kaufman, J. D. Foster, P. Nuyujukian, S. I. Ryu, and K. V. Shenoy, “Neural population dynamics during reaching,” *Nature*, vol. 487, no. 7405, pp. 51–56, 2012.
- [49] G. F. Elsayed, A. H. Lara, M. T. Kaufman, M. M. Churchland, and J. P. Cunningham, “Reorganization between preparatory and movement population responses in motor cortex,” *Nature Communications*, vol. 7, no. 1, art. no. 13239, 2016.
- [50] R. D. Flint, M. R. Scheid, Z. A. Wright, S. A. Solla, and M. W. Slutzky, “Long-term stability of motor cortical activity: Implications for brain machine interfaces and optimal feedback control,” *Journal of Neuroscience*, vol. 36, no. 12, pp. 3623–3632, 2016.
- [51] V. Mante, D. Sussillo, K. V. Shenoy, and W. T. Newsome, “Context-dependent computation by recurrent dynamics in prefrontal cortex,” *Nature*, vol. 503, no. 7474, pp. 78–84, 2013.
- [52] S. Fusi, E. K. Miller, and M. Rigotti, “Why neurons mix: high dimensionality for higher cognition,” *Current Opinion in Neurobiology*, vol. 37, pp. 66–74, 2016.
- [53] A. Parthasarathy, R. Herikstad, J. H. Bong, F. S. Medina, C. Libedinsky, and S.-C. Yen, “Mixed selectivity morphs population codes in prefrontal cortex,” *Nature Neuroscience*, vol. 20, no. 12, pp. 1770–1779, 2017.